

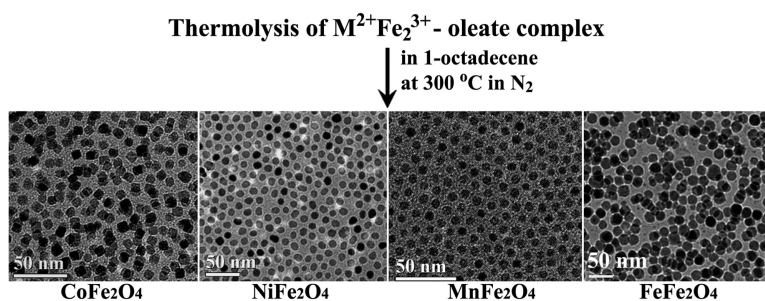
Communication

A Facile Thermolysis Route to Monodisperse Ferrite Nanocrystals

Ningzhong Bao, Liming Shen, Yuhsiang Wang, Prahallad Padhan, and Arunava Gupta

J. Am. Chem. Soc., **2007**, 129 (41), 12374-12375 • DOI: 10.1021/ja074458d • Publication Date (Web): 20 September 2007

Downloaded from <http://pubs.acs.org> on February 14, 2009



More About This Article

Additional resources and features associated with this article are available within the HTML version:

- Supporting Information
- Links to the 6 articles that cite this article, as of the time of this article download
- Access to high resolution figures
- Links to articles and content related to this article
- Copyright permission to reproduce figures and/or text from this article

[View the Full Text HTML](#)

A Facile Thermolysis Route to Monodisperse Ferrite Nanocrystals

Ningzhong Bao,* Liming Shen, Yuhsiang Wang, Prahallad Padhan, and Arunava Gupta*
Center for Materials for Information Technology, University of Alabama, Tuscaloosa, Alabama 35487

Received June 19, 2007; E-mail: nzhbao@mint.ua.edu; agupta@mint.ua.edu

Monodisperse inorganic nanocrystals have been intensively investigated in recent years, both because of fundamental scientific interest and technological applications arising from the unique properties in reduced dimension.¹ In particular, the spinel ferrites of composition MFe_2O_4 ($M = Co, Ni, Mn, Fe, \text{etc.}$) exhibit interesting magnetic, magnetoresistive, and magneto-optical properties that are potentially useful for a broad range of applications.² Their magnetic properties can be systematically varied by changing the identity of the divalent M^{2+} cation or by partial substitution while maintaining the basic crystal structure.² The properties can be additionally tuned by controlling the shape, size, and crystallinity of the nanocrystals. For biomedical application, the use of spherical ferrite nanocrystals with a smooth surface, narrow size distribution, and high magnetic moment is desirable.³ On the other hand, monodisperse ferrite nanocrystals with a preferential magnetic easy axis direction are needed for nanodevice and data storage applications. Thus, a simple and cost-effective synthesis route for large-scale production of monodisperse ferrite nanocrystals, with tunable shapes and sizes, would be very attractive for practical applications.

Considerable effort has been devoted to preparing monodisperse ferrite nanocrystals with controlled size and shape. A range of methods, including alkali reduction,⁴ reverse micelles,⁵ and coprecipitation⁶ have been reported. However, the obtained product often suffers from particle agglomeration and a broad size distribution. In order to obtain monodisperse nanoparticles, suitable precursor systems that can generate stable monomers in solution are necessary. One of the more successful routes involves thermal decomposition of mixed organic M^{2+} and Fe^{3+} compounds, such as metal acetylacetonates, metal carbonyls, etc., in high boiling point solvents. In combination with the use of surfactants, such as oleic acid and oleyl amine, this procedure results in the formation of monodisperse ferrite nanoparticles with good crystallinity and uniform size.⁷ Herein, we report on the synthesis of ferrite nanocrystals using a simpler route that involves decomposition of mixed metal-oleate complexes formed via low-temperature reaction of the constituent metal halides with sodium oleate. The synthesis of binary metal oxides through thermolysis of metal-oleate complexes has been reported.⁸ However, the synthesis of ternary compounds using metal-oleate complexes has thus far been limited to copper-indium sulfide nanocrystal heterostructures. In this case, segregation of Cu_2S and In_2S_3 leads to the formation of interesting heterostructure nanocrystals of various shapes.⁹ This behavior can be attributed to the differences in the decomposition temperature of the Cu- and In-oleate. We report on the synthesis of monodisperse nanocrystals of a number of spinel ferrites with uniform composition by thermolysis of a mixed binary metal-oleate precursor. The choice of an intimately mixed precursor with similar decomposition temperature of the constituent oleates is critical for the compositional and structural uniformity of the nanocrystals.

Monodisperse MFe_2O_4 nanocrystals were obtained by thermolysis of the $M^{2+}Fe_2^{3+}$ -oleate complex dissolved in 1-octadecene at 300 °C under N_2 (see SI for details). The size and shape of the synthesized MFe_2O_4 nanocrystals were investigated using transmis-

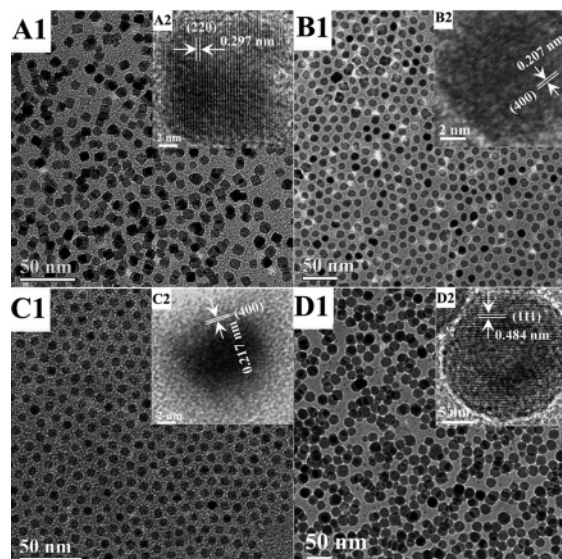


Figure 1. TEM images of MFe_2O_4 nanocrystals: (A1) $CoFe_2O_4$; (B1) $NiFe_2O_4$; (C1) $MnFe_2O_4$; (D1) $FeFe_2O_4$ (Fe_3O_4). The corresponding high-resolution TEM image of the individual nanocrystals is shown in the inset.

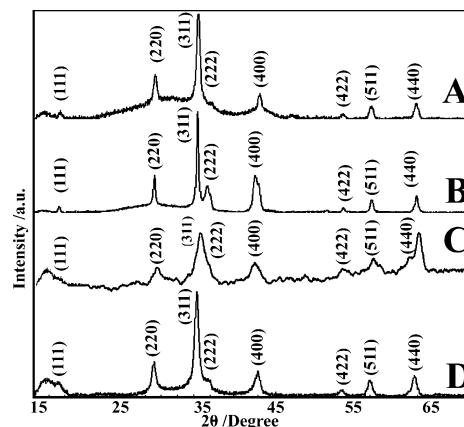


Figure 2. XRD patterns of MFe_2O_4 nanocrystals: (A) $CoFe_2O_4$; (B) $NiFe_2O_4$; (C) $MnFe_2O_4$; (D) $FeFe_2O_4$ (Fe_3O_4).

sion electron microscopy (TEM). Figure 1 shows representative images of four different ferrites. The shape and average size vary from cubic for 9 nm $CoFe_2O_4$ (Figure A1), near-spherical for 11 nm $NiFe_2O_4$ (Figure B1), and perfectly spherical for both 7 nm $MnFe_2O_4$ (Figure C1) and 24 nm $FeFe_2O_4$ (Figure D1). All of the products have narrow size distributions (see Figure S11). The insets show the high-resolution images of the various ferrites. Lattice fringes corresponding to a group of atomic planes within each particle are clearly visible, indicating the single crystalline nature of the nanocrystals. The crystallinity and structure of the MFe_2O_4 nanocrystals were also confirmed by powder X-ray diffraction (XRD). As shown in Figure 2, the peak position and relative intensity of all diffraction peaks for the four products match

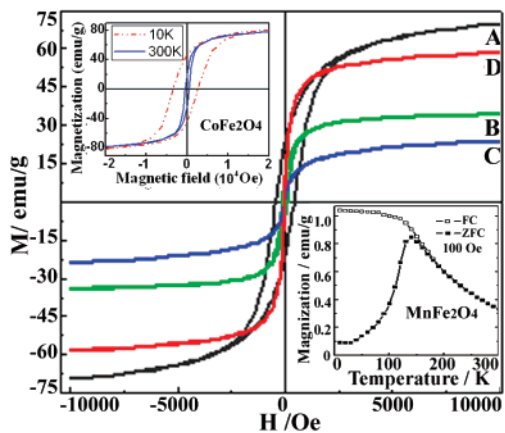


Figure 3. Room-temperature magnetic hysteresis of $M\text{Fe}_2\text{O}_4$ nanocrystals: (A) CoFe_2O_4 ; (B) NiFe_2O_4 ; (C) MnFe_2O_4 ; (D) FeFe_2O_4 (Fe_3O_4). The insets are hysteresis loops of CoFe_2O_4 measured at 10 and 300 K (top), and zero-field-cooled (ZFC) and field-cooled (FC) magnetization of MnFe_2O_4 measured in an applied field of 100 Oe (bottom).

well with standard powder diffraction data. From the peak widths, the average crystalline size is estimated to be 10.4 nm for CoFe_2O_4 , 12.6 nm for NiFe_2O_4 , 7.8 nm for MnFe_2O_4 , and 20.2 nm for FeFe_2O_4 , agreeing with the TEM results.

The room-temperature hysteresis loop of the ferrites was measured using a vibrating sample magnetometer (VSM). The magnetization curves, as shown in Figure 3, display relatively high saturation magnetization. The magnetic saturation values of CoFe_2O_4 , NiFe_2O_4 , and FeFe_2O_4 are 69.7, 34.2, and 58.6 emu/g, respectively, close to the theoretical values of 71.2, 47.5, and 96.2 emu/g. The observed values are within the range reported in the literature.^{2,4–6} However, the MnFe_2O_4 nanocrystals exhibit a low saturation magnetization of 23.9 emu/g, which is much smaller than the theoretical values of 120.8 emu/g. The reduced saturation magnetization of ferrite nanocrystals is generally believed to be due to the decreased particles size and presence of a magnetic dead or antiferromagnetic layer on the surface.¹⁰ As indicated by the ZFC-FC curves in the inset of Figure 3, the MnFe_2O_4 has a low blocking temperature (~ 140 K) as compared with that of other ferrites (Figure SI2). This is because of the smaller size and lower Curie temperature (~ 300 °C in the bulk) than the other ferrites. Other than CoFe_2O_4 , the hysteresis loops for the other ferrites display very low coercivities, with no remanence, as would be expected for superparamagnetic behavior. Despite the relatively small size, the CoFe_2O_4 nanocrystals display a markedly high coercivity of 430 Oe at room temperature and 3000 Oe at 10 K. This is likely because of its higher magnetocrystalline anisotropy because of spin-orbit contribution as compared to the other ferrites. On the basis of Langevin fits to the magnetization loops, the size of superparamagnetic MnFe_2O_4 and FeFe_2O_4 nanocrystals is estimated to be 5.2 and 19.8 nm, respectively.

The formation of ferrites by thermal decomposition was investigated by TGA. The TGA curves (Figure SI3) of the different mixed (Co, Ni, and Mn)²⁺ Fe_2^{3+} -oleate complexes show a small weight loss below 300 °C and a much larger and rapid weight loss of ~ 300 °C due to the decomposition of the oleate complex. For the formation of monodisperse spinel nanocrystals with homogeneous composition, it is important that the binary oleates are intimately mixed and have similar decomposition temperatures. The latter is illustrated by our inability to synthesize CuFe_2O_4 using the oleate route. Using a mixed $\text{Cu}^{2+}\text{Fe}_2^{3+}$ -oleate complex, we observed the formation of red Cu nanoparticles at ~ 250 °C, and the color of reaction solution changed to dark brown at 300 °C

due to the subsequent formation of iron oxide, as confirmed by the XRD (Figure SI4) and TEM (Figure SI5) data. TGA analysis shows weight loss over a relatively broad temperature range, with weight losses at low and high temperatures corresponding to the decomposition of Cu^{2+} -oleate and Fe^{3+} -oleate, respectively (Figure SI6). Besides differences in the decomposition temperature, the component oxides are favored because of the thermodynamic instability of CuFe_2O_4 relative to CuO and Fe_2O_3 at low temperatures. The differences in the decomposition temperature are also the likely cause for the separate formation of Cu_2S and In_2S_3 , instead of CuInS_2 , from a mixed $\text{Cu}^{1+}\text{In}^{3+}$ -oleate complex.⁹ The intimate mixing achieved by synthesis of the mixed metal oleates from the halides is important for monodispersity. This is indicated by comparison with synthesized CoFe_2O_4 (Figures SI7 and 8) for which the Co^{2+} - and Fe^{3+} -oleate were prepared separately and then mixed together for the reaction. A broader shape and size distribution is obtained in this case as compared to a premixed metal oleate complex.

In summary, we have demonstrated the synthesis of monodisperse ternary ferrite nanocrystals of uniform composition through a facile thermolysis of well-organized $\text{M}^{2+}\text{Fe}_2^{3+}$ -oleate complexes in which the M^{2+} -oleate and Fe^{3+} -oleate have close decomposition temperatures, using nontoxic and inexpensive reactants.

Acknowledgment. This work was supported by NSF under Grant No. ECS-0621850. The authors are grateful to J. Weston, M. Smiglak, L. Wen, S. Bhattacharyya, and Y. Hou for experimental assistance and technical discussions.

Supporting Information Available: Experimental details and Figures SI1–8. This material is available free of charge via the Internet at <http://pubs.acs.org>.

References

- (1) (a) Lu, A. H.; Salabas, E. L.; Schuth, F. *Angew. Chem., Int. Ed.* **2007**, *46*, 1222–1244. (b) Yin, Y.; Alivisatos, A. P. *Nature* **2005**, *437*, 664–670.
- (2) (a) Sugimoto, M. *J. Am. Ceram. Soc.* **1999**, *82*, 269–280. (b) Yu, S.; Yoshimura, M. *Chem. Mater.* **2000**, *12*, 3805–3810. (c) Abe, M.; Tada, M.; Matsushita, N.; Shimada, Y. *J. Appl. Phys.* **2006**, *99*, 08M907. (d) Kim, C.; Lee, J.; Katoh, S.; Murakami, R.; Yoshimura, M. *Mater. Res. Bull.* **2001**, *36*, 2241–2250. (e) Subramani, A.; Matsushita, N.; Watanabe, T.; Tada, M.; Abe, M.; Yoshimura, M. *J. Appl. Phys.* **2007**, *101*, 09M504. (f) Park, J.; Joo, J.; Kwon, S.; Jang, Y.; Hyeon, T. *Angew. Chem., Int. Ed.* **2007**, *46*, 4630–4660. (g) Wang, X.; Zhuang, J.; Peng, Q.; Li, Y. *Nature* **2005**, *437*, 121–124.
- (3) (a) Sun, Y.; Xia, Y. *Science* **2002**, *298*, 2176–2179. (b) Wang, Y. L.; Xia, Y. N. *Nano Lett.* **2004**, *4*, 2047–2050. (c) Gee, S. H.; Hong, Y. K.; Erickson, D. W.; Park, M. H. *J. Appl. Phys.* **2003**, *93*, 7560–7562.
- (4) Mooney, K. E.; Nelson, J. A.; Wagner, M. J. *Chem. Mater.* **2004**, *16*, 3155–3161.
- (5) (a) Liu, C.; Zou, B.; Rondinone, A. J.; Zhang, Z. J. *J. Am. Chem. Soc.* **2000**, *122*, 6263–6267. (b) Lee, Y.; Lee, J.; Bae, C. J.; Park, J. G.; Noh, H. J.; Park, J. H.; Hyeon, T. *Adv. Funct. Mater.* **2005**, *15*, 503–509.
- (6) Zhang, Z. J.; Wang, Z. L.; Chakoumakos, B. C.; Yin, J. S. *J. Am. Chem. Soc.* **1998**, *120*, 1800–1804.
- (7) (a) Sun, S.; Zeng, H. *J. Am. Chem. Soc.* **2002**, *124*, 8024–8205. (b) Sun, S.; Zeng, H.; Robinson, D. B.; Raoux, S.; Rice, P. M.; Wang, S. X.; Li, G. *J. Am. Chem. Soc.* **2004**, *126*, 273–279. (c) Zeng, H.; Rice, P. M.; Wang, S. X.; Sun, S. *J. Am. Chem. Soc.* **2004**, *126*, 11458–11459. (d) Song, Q.; Zhang, Z. J. *J. Am. Chem. Soc.* **2004**, *126*, 6164–6168. (e) Vestal, C. R.; Song, Q.; Zhang, Z. J. *J. Phys. Chem. B* **2004**, *108*, 18222–18227. (f) Tirosh, E.; Shemer, G.; Markovich, G. *Chem. Mater.* **2006**, *18*, 465–470.
- (8) (a) Park, J.; An, K.; Hwang, Y.; Park, J. G.; Noh, H. J.; Kim, J. Y.; Park, J. H.; Hwang, N. M.; Hyeon, T. *Nat. Mater.* **2004**, *3*, 891–895. (b) An, K.; Lee, N.; Park, J.; Kim, S. C.; Hwang, Y.; Park, J. G.; Kim, J. Y.; Park, J. H.; Han, M. J.; Yu, J.; Hyeon, T. *J. Am. Chem. Soc.* **2006**, *128*, 9753–9760. (c) Jana, N. R.; Chen, Y.; Peng, X. *Chem. Mater.* **2004**, *16*, 3931–3935. (d) Hyeon, T. *Chem. Commun.* **2003**, 927–934.
- (9) Chio, S. H.; Kim, E. G.; Hyeon, T. *J. Am. Chem. Soc.* **2006**, *128*, 2520–2521.
- (10) (a) Geng, B. Y.; Ma, J. Z.; Liu, X. W.; Du, Q. B.; Kong, M. G.; Zhang, L. D. *Appl. Phys. Lett.* **2007**, *90*, 043120. (b) Zheng, M.; Wu, X. C.; Zou, B. S.; Wang, Y. *J. Magn. Magn. Mater.* **1998**, *183*, 152–156. (c) Pankhurst, Q. A.; Pollard, R. J. *Phys. Rev. Lett.* **1991**, *67*, 248–250.

JA074458D